Methylene blue reduces Aβ levels and rescues early cognitive deficit by increasing proteasome activity

David X. Medina, **Antonella Caccamo**, and **Salvatore Oddo**[*]
Department of Physiology and The Barshop Institute for Longevity and Aging Studies, University of Texas Health Science Center at San Antonio, 7703 Floyd Curl Drive, San Antonio, TX 78229

Abstract

Promising results have emerged from a phase II clinical trial testing Methylene blue (MB) as a potential therapeutic for Alzheimer disease (AD), where improvements in cognitive functions of AD patients after 6 months of MB administration have been reported. Despite these reports, no preclinical testing of MB in mammals has been published, and thus its mechanism of action in relation to AD pathology remains unknown. In order to elucidate the effects of MB on AD pathology and to determine its mechanism of action, we used a mouse model (3xTg-AD) that develops age-dependent accumulation of Aβ and tau and cognitive decline. Here, we report that chronic dietary MB treatment reduces Aβ levels and improves learning and memory deficits in the 3xTg-AD mice. The mechanisms underlying the effects of MB on Aβ pathology appears to be mediated by an increase in Aβ clearance as we show that MB increases the chymotrypsin-and trypsin-like activities of the proteasome in the brain. To our knowledge, this is the first report showing that MB increases proteasome function and ameliorates AD-like pathology *in vivo*. Overall, the data presented here support the use of MB for the treatment of AD and offer a possible mechanism of action.

INTRODUCTION

Alzheimer disease (AD), the most common cause of dementia with 5.5 million Americans affected, is an age-dependent disorder that leads to declines in cognitive ability, including memory loss (29). Neuropathologically, AD is characterized by the accumulation of neurofibrillary tangles (NFTs), composed of hyperphosphorylated tau protein, and neuritic plaques, mainly composed of aggregated amyloid-β (Aβ) peptide (29). Aβ is the result of sequential cleavage of the amyloid precursor protein (APP), generating two major fragments $A\beta_{40}$ and $A\beta_{42}$, the latter being more prone to aggregation and comprises most of the Aβ in plaques (29).

Strong evidence suggests that the accumulation of Aβ plays a major role in AD pathogenesis (10). Aβ can accumulate because of an increase in its production or a decrease in its degradation. Along these lines, different laboratories aim at preventing Aβ production or increasing its degradation in the design of disease-modifying therapies (8). While various proteases are shown to directly cleave Aβ, the two major intracellular quality control systems, the ubiquitin proteasome system and the autophagy-lysosome system, also play a role in Aβ turnover (5,15). Indeed, several studies have reported decreased proteasome activity and autophagy dysfunction in AD brains and in animal models (5,13,28).

---

[*]*To whom correspondence should be addressed:* SALVATORE ODDO, Ph.D. Assistant Professor Department of Physiology University of Texas Health Science Center, San Antonio 7703 Floyd Curl Drive San Antonio, TX 78229-3900 Tel: 210-567-4340 Fax: 210-567-4410 oddo@uthscsa.edu.

Methylene blue (MB), a member of the phenothiazine family (Fig. 1A), has been used for more than 100 years in the treatment of various diseases including malaria and urinary tract infections (25). MB crosses the blood-brain barrier and has been shown to have high bioavailability to the brain (27). MB blue has been shown to exhibit effects on several cellular targets including NO synthase, cythochrome c oxidase, and the 70-kDa heat shock protein (1,7,12,25,33). Additionally, MB reduces Aβ oligomers levels and prevents tau aggregation, *in vitro* (14,35). Similarly, acute administration of MB to organotypic slices derived from transgenic mice expressing mutant human tau reduces tau levels and phosphorylation (12). In contrast, however, a recent *in vivo* study showed that MB administration failed to reduce tau phosphorylation and aggregation in transgenic zebrafish expressing mutant human tau (32). More important, the outcome of a phase II clinical trial of MB treatment for AD has shown encouraging results as significant improvement in cognitive functions was reported for patients on MB compared to patients on placebo (9). Taken together these data indicate that MB may be a new potential drug for the treatment of AD; however, no preclinical testing of MB in mammals has been conducted, and its mechanism of action in relation to AD pathology remains unknown. Therefore, there is an urgent need for studies aimed at determining the mechanism of action of MB in relation to AD.

To evaluate putative AD therapies, mouse models have proven to be highly valuable (34,36). Thus, in order to elucidate the effects of MB on AD pathology and determine its mechanism of action, we used a mouse model (known as the 3xTg-AD mice) that mimics several aspects of AD including the age-dependent Aβ and tau pathology and cognitive decline (17,19,21,22) The development of both Aβ and tau pathology make the 3xTg-AD mice an highly desirable model for the evaluation of putative therapeutic drugs, as a compound may have opposite effects on Aβ and tau pathology (16,18). Here, we examined the effects of chronic dietary MB treatment on AD-like pathology and the associated cognitive decline in 3xTg-AD mice.

MATERIAL AND METHODS

Mice and MB treatment

The derivation and characterization of the 3xTg-AD mice has been described elsewhere (19). The control diet was made by grinding food pellets into a fine powder using a food processor; 2 g of sucrose were added per 100 g of food powder. For MB supplemented food, 25 mg of MB (Fig. 1A), USP grade (ScienceLab.com, Houston, TX) were added per 100 g of control diet. Food was placed in feeding dishes in mouse cages and was replaced with fresh food daily. Mice had *ad libitum* access to food and water.

Behavioral testing

Morris water maze testing was conducted as described previously (22). Briefly, mice were given 4 training trials per day per 5 day in a circular pool of 90 cm in diameter. The mice were to find a submerged platform (1.5 cm below the water surface) by using cues placed on the walls. Notably, the platform was not visible to the mice as the water was rendered opaque by the addition of white non-toxic paint. Twenty-four hours after the last training trails, mice were replaced in the pool without the platform and left free to swim for 60 seconds. The training and probe trials were recorded by a video camera mounted on the ceiling, and data were analyzed using the EthoVisioXT tracking system.

Protein Extraction, Western Blot, and ELISA

All mice behaviorally tested were killed and analyzed for the biological studies listed below. Specifically, mice were killed by CO_2 asphyxiation and their brains extracted and cut in half

sagitally. For immunohistochemical analysis, one-half was drop-fixed in 4% paraformaldehyde in phosphate-buffered saline for 48 hours and then transferred in 0.02% sodium azide in phosphate-buffered saline until slicing. The other half was frozen in dry ice for Western blot analysis. Toward this end, after removing the cerebellum, frozen forebrains were homogenized in a solution of tissue protein extraction reagent (Pierce, Rockford, IL) containing 0.7 mg/ml of Pepstatin A supplemented with a complete Mini protease inhibitor tablet (Roche, Mannheim, Germany) and phosphatase inhibitors (Invitrogen, Carlsbad, CA). The homogenized mixtures were briefly sonicated to sheer the DNA and centrifuged at 4 °C for 1 hour at 100,000 g. The supernatant was stored as the soluble fraction. The pellet was re-homogenized in 70% formic acid and centrifuged as above. The supernatant was stored as the insoluble fraction. For Western blot analyses and ELISA measurements were conducted as described in (22). For the Western blots, 5 or more different samples from each genotype and treatment group were used. The voltage dependent anion channel (VDAC) was used as loading control for the COX blots, while β-actin was used as loading control for all other blots.

Immunohistochemistry

Thirty μm-thick brain sections were obtained using a Leica vibratome slicing system, and sections were stored at 4°C in 0.02% sodium azide in phosphate-buffered saline. Immunostaining experiments were conducted as described in (4).

Antibodies

Anti COX-IV, 1:1000 (Cell Signaling, Danver, MA); anti VDAC, 1:1000 (Cell Signaling); anti-APP 6E10, 1:3000 (Chemicon Temecula, CA); anti tau HT-7, 1:3000 (Pierce Rockford, IL); anti tau AT270, 1:1000 (Biosource Camarillo, CA); anti-Aβ, 1:200 (Biosource); anti ATG-7, 1:1000 (Cell Signaling); anti LC3B, 1:1000 (Cell Signaling); anti Beclin, 1:1000 (Cell Signaling). All of these antibodies are faily specific and widely used (17,20,26,28,39).

Proteasome activity assay

Proteasomal activity was assayed by incubating 10 μl of brain homogenate with 75 μM proteasomal substrates Suc-LLVY-AMC, Bz-VGR-AMC and Z-LLE-AMC (Enzo Life Sciences, Plymouth Meeting, PA), which probe for chymotrypsin-like, trypsin-, and peptidylglutamyl-peptide hydrolyzing-like (PGPH) activities, respectively. Reactions were carried out in assay buffer (25mM HEPES, pH 7.5, 0.5mM EDTA, 0.05% NP-40) in a total of 200 μl in black 96-well plates. Substrates were added immediately prior to readings. Kinetic readings were taken at 37°C every 1.5 min for 60 min (excitation 360 nm, emission 460 nm) using the Synergy HT multi-mode microplate reader using the Gen5 software (BioTek, Winooski, VT). Readings were normalized to protein concentration.

Preparation of isolated mitochondria

Mitochondria were isolated using protocol from (11). MB treated and untreated 3xTg-AD and NonTg mice were killed by decapitation and brains were quickly dissected on a chilled petri dish. After removing the cerebellum, the brain was divided into hemispheres. One hemisphere was frozen and stored at −80° C for future biochemical analysis, and the second hemisphere was minced and washed with ice-cold isolation buffer (210 mM mannitol, 70mM sucrose, 10 mM HEPES, 1mM EDTA, 0.45% BSA, 0.5mM DTT, and EDTA free complete mini protease inhibitor mixture tablets). The tissue sample was gently homogenized in 2 ml buffer using a glass homogenizer (15 strokes). The resulting homogenate was centrifuged at 1,450 × g for 7 min at 4° C to remove nuclei and tissue particles. The supernatant was placed in a new tube and the low speed centrifugation was repeated once. The supernatant was then removed, placed in a new tube, and centrifuged at

10,000 × g for 5 min at 4° C to pellet the mitochondria. The supernatant was stored for analysis as a cytosolic franction. The mitochondrial pellet was then resuspended in 1 ml of ice cold isolation buffer, and centrifuged at 830 × g for 3 min at 4° C. The supernatant was centrifuged at 10,000 × g for 5 min at 4° C to collect the final mitochondria fraction. The supernatant was discarded and the mitochondrial pellet was resuspended in 200 μl of ice cold buffer. Isolated mitochondria were used immediately after preparation.

Free ATP levels and ATP production

ATP levels were measured from cytosolic fraction prepared during mitochondrial isolation. ATP levels were taken using the ATP Bioluminescence Assay Kit CLSII (Roche, Mannheim, Germany) according to manufacturer's instructions. In brief, 10 μl of cytosolic fraction plus 40 μl of PBS were added to each well in duplicate. Luciferase reagent was added to wells to final volume of 100 μl and luminescence was measured using the BioTek SynergyHT multimode microplate reader in the luminescence mode. Measurements, taken over 15 min, were normalized to protein concentration. ATP production was measured using ATP Bioluminescence Assay Kit CLSII (Roche, Mannheim, Germany) according to the manufacturer's instructions.

Cytochrome c oxidase activity and levels

Cytochrome c oxidase (COX) levels were measured by Western blot using an antibody against COX IV subunit of COX. COX activity was measured using Cytochrome c Oxidase Assay Kit (Sigma, St. Louis, MO) according to manufacturer's instructions. Briefly, 5μl of mitochondrial fraction was added to 1.1 ml of reaction solution that contained 50μl of 0.22 mM fully reduced ferrocytochrome c by 0.1M DTT. Activity was calculated by measuring the decrease of absorbance at 550 nm was recorded for a 1-min reaction at 10-seconds intervals. Measurements were normalized to protein concentration.

Statistical analyses

Statistical analyses were conducted using multifactor analysis of variance, following by post hoc Bonferoni test to determine individual difference among groups. Student *t* test where used when suitable.

RESULTS

To evaluate the effects of MB (Fig. 1A) on AD-like pathology, we treated 6-month-old males NonTg (n=13) and 3xTg-AD (n=17) mice with a 0.025% w/w MB supplemented diet, provided *ad libitum* for 16 weeks (Fig. 1B). Additionally, age- and gender-matched NonTg (n=10) and 3xTg-AD (n=14) mice were fed the control diet, which was prepared as described in the methods section. The concentration of MB was chosen based on previous reports (3). Mice were monitored daily for general health, and no observable adverse effects were detected. As mice were grouped housed, we could not measure the individual amount of food intake. However, the body weight of mice was monitored weekly, and no significant differences were observed among the groups throughout the treatment period (Table 1).

Methylene Blue improves learning and memory in 3xTg-AD mice

After 8 and 16 weeks of treatment, we evaluated the effects of MB on learning and memory using the spatial references version of the Morris water maze (MWM). This task was chosen because it mainly relays on the hippocampus, a brain region showing severe Aβ and tau pathology in AD patients and in the 3xTg-AD mice (29). Indeed, the 3xTg-AD mice show hippocampal-dependent learning and memory deficits (2,22). The mice were maintained on their respective diets throughout the behavioral testing period. To measure spatial learning,

mice were given 4 training trials per day for 5 days. During the first behavioral testing conducted 8 weeks after the beginning of the treatment, we observed no changes in learning and memory between the mice on MB and the genotyped-matched mice on the control diet (data not shown). After 16 weeks of treatment, all mice were retested in the MWM. To avoid *savings* from the previous exposures to the task, we changed the extramaze cues and the location of the platform. We found that on day 4 of training, the MB-treated 3xTg-AD mice performed significantly better than the 3xTg-AD mice on the control diet (Fig. 1C; $p < 0.05$). No statistically significant changes were observed among any of the groups during any of the other days of training, including after 5 days of training. While the reason for this is not completely clear, the lack of statistical difference on day 5 could be attributed to a plateau effect in the control mice. Indeed the rate of improvement in the control mice declines on day 5 (Fig. 1 C). Notably, the treated 3xTg-AD mice performed as well as both NonTg groups (Fig. 1C). Twenty-four hours after the last training trial, we conducted probe trials and found that the 3xTg-AD mice treated with MB reached the platform location significantly faster compared to the 3xTg-AD mice on the control diet (Fig. 1D). Similarly, the number of platform location crosses and time spent in the target quadrant was significantly increased for the MB-treated 3xTg-AD mice compared to 3xTg-AD mice on the control diet (Fig. 1E–F). Notably, the MB-treated 3xTg-AD mice performed similar to NonTg mice by all measures. Finally, we found that the MB-treated NonTg mice performed as well as NonTg mice on the control diet (Fig. 1D–F). Although it remains to be determined as to why 8 weeks of MB administration had no effects on learning and memory, it is tempting to speculate that a shorter treatment period may not be sufficient to reduce Aβ levels. Overall, our data indicate that under the conditions used here, MB treatment rescues spatial memory in the 3xTg-AD mice.

MB treatment does not affect mitochondrial function

At the end of the behavioral testing, all mice were killed and their brains processed for neuropathological and biochemical evaluation. MB has been demonstrated to increase mitochondrial function *in vitro* and *in vivo* (1,6). This is especially relevant as mitochondrial function has been demonstrated to be reduced in AD patients as well as in several transgenic mouse models (11,30,38). To determine the effects of MB treatment on mitochondria, we first measured cytochrome c oxidase levels and its activity and found no significant changes in the brains of the MB-treated 3xTg-AD mice compared to 3xTg-AD mice on the control diet (Fig. 2A–C). We next measured free ATP levels from the cytosolic fraction of homogenized brains and ATP production in mitochondrial enriched fractions (see methods section), finding no differences in ATP levels or ATP production between the MB-treated and control 3xTg-AD mice (Fig. 2D). Although the possibility that different concentrations of MB could elicit a change in mitochondrial function cannot be excluded, our results show that under the conditions used here, MB does not cause significant changes in brain mitochondrial function in the 3xTg-AD mice.

MB reduces Aβ but not tau levels

To determine the consequences of MB treatment on Aβ pathology, we quantitatively measured Aβ levels by sandwich ELISA. Notably, we found that soluble $A\beta_{40}$ and $A\beta_{42}$ levels were significantly reduced in the brains of the MB-treated 3xTg-AD mice compared to the 3xTg-AD mice on the control diet (Fig. 3A–B). Conversely, insoluble $A\beta_{40}$ and $A\beta_{42}$ levels were not changed by the MB treatment (Fig. 3A–B). Although MB significantly decreased the steady-state levels of Aβ, we found no changes in Aβ immunoreactivity in the brains of treated and untreated mice as detected by 6E10 and Aβ42 specific antibodies (Fig. 3C–D and data not shown). Further studies are needed to understand the reasons behind this apparent discrepancy; however, it is tempting to speculate that 16 weeks of MB treatment, at

the dose used here, is not enough to affect Aβ accumulation and that a longer treatment may generate a different outcome on Aβ deposits.

In addition to Aβ accumulation, the 3xTg-AD mice develop an age-dependent accumulation of phosphorylated and aggregated tau (17). Specifically, at 10 months of age, tau in the 3xTg-AD mice is hyperphosphorylated at Thr212 and Ser214 (as detected by the AT100 antibody), at Thr181 (as detected by the AT270 antibody), and Ser202 and Thr205 (as detected by the AT8 antibody; (17,22)). To determine the effects of MB treatment on tau pathology, we compared the accumulation and phosphorylation of tau between the MB-treated and control 3xTg-AD mice. For our analysis, we focused on the hippocampus as we have previously showed that tau is highly hyperphosphorylated in CA1 pyramidal neurons (17,22). Using Western blot analysis, we found that MB treatment did not alter the steady-state levels of phosphorylated tau as detected by the antibody AT270 (Fig. 4A–B). To determine whether MB had any effect on tau mislocalization, we stained brain sections from MB-treated and control 3xTg-AD mice with the human specific anti-tau antibody HT7. Consistent with the biochemical data, we found that MB had no effect on somatodendritic tau accumulation (Fig. 4C–D). These results are in agreement with recent data demonstrating abnormal tau phosphorylation is not affected by MB treatment in a transgenic zebrafish overexpressing mutant human tau (32).

MB increases proteasome activity

Steady-state levels of Aβ are the result of the equilibrium between production and degradation. To determine the mechanism responsible for the reduction in Aβ following MB administration, we initially determined whether the decrease in Aβ levels was due to changes in its production by analyzing APP processing by Western blot. We first measured the steady-state levels of APP using the antibody 6E10, finding that APP levels showed no alterations between the MB-treated and the control 3xTg-AD mice (Fig. 5A–B). Subsequently, we measured the levels of C99 and C83, the two major C-terminal derivatives of APP, using a C-terminal-specific APP antibody. We found that levels of C99 and C83 were not changed in the MB-treated 3xTg-AD mice compared to the 3xTg-AD mice on the control diet (Fig. 5A–B). These data suggest that the MB-mediated decrease in Aβ levels is not due to changes in its production.

We next determined whether the MB effects on Aβ were mediated by an increase in its degradation via the two major intracellular quality control systems involved in protein turnover, the ubiquitin-proteasome system and the autophagic system. To determine whether MB increases autophagy induction, we measured the levels of autophagy-related proteins Atg7, Beclin 1 (which are necessary for autophagy induction) and LC3-II. The latter is commonly used to measure the levels of autophagy induction as it is derived from LC3-I during autophagy induction and incorporated into the growing membrane of autophagosomes (24). We found that MB did not alter autophagy induction as the levels of Beclin 1, Atg 7, and LC3 were not significantly different between the 3xTg-AD mice on MB and the 3xTg-AD mice on the control diet (Fig. 5C–D).

Proteasomal dysfunction has been implicated in AD pathology in both human and animal models (13,31). Furthermore, previous reports have shown that MB decreases Hsp70 activity, which is involved in protein degradation and proteasome activity (12,33). To investigate whether changes in proteasomal activity may mediate the MB-effect on Aβ, we utilized fluorogenic substrates Bz-VGR-AMC, Suc-LLVY-AMC, and Z-LLE-AMC to measure trypsin-like, chymotrypsin-like, and peptidylglutamyl-peptide hydrolyzing (PGPH) activities of the proteasome in the brains of treated and untreated 3xTg-AD mice. While no significant changes were observed in the caspase-like activity between the two groups (Fig. 5G), we found a significant increase in the trypsin-like activity in the brains of the 3xTg-AD

mice following MB treatment (Fig. 4F). Similarly, MB significantly increased the chymotrypsin-like activity (Fig. 5E). Although further studies are needed to elucidate the mechanisms by which MB increases proteasome activity, taken together our data provide strong supporting evidence for a proteasomal involvement in the MB-mediated decrease in soluble Aβ levels and the associated cognitive deficits.

Discussion

In vitro evidence from various laboratories demonstrated that MB inhibits the formation of inclusions made of different proteins, including Aβ oligomers, tau, and TDP-43 (9,35,37). A recent *in vivo* study also highlighted the ability of MB to prevent aggregation and deposition of polyglutamine in Zebrafish (32). More important, the results of a recent phase II clinical trial showed that MB arrests disease progression in mild and moderate AD cases over 50 weeks (9). Despite the results of the clinical trial, no preclinical work in mammals has been reported. Therefore, there is an urgent need for studies aimed at addressing the mechanism of action of MB in relation to AD. Toward this end, transgenic models of AD are a valuable tool. In this study, we show that 16 weeks of MB administration improved learning and memory deficits in 3xTg-AD mice, consistent with the results of the phase II clinical trial.

The early learning and memory deficits in the 3xTg-AD mice are due to accumulation of soluble Aβ (2,22). Indeed, we have previously shown that small decreases in soluble Aβ levels are sufficient to ameliorate learning and memory deficits in young but not in old 3xTg-AD mice, where the behavioral deficits are exacerbated by the concomitant development of tau pathology (2,22,23). Consistent with these reports, here we show that MB-mediated decreases in soluble Aβ levels are sufficient to rescue early learning and memory deficits in the 3xTg-AD mice. Although we cannot exclude that other pathways may be involved, the mechanism underlying the decrease in Aβ levels appears to be mediated by an increase in proteasome function. Toward this end, here we show no changes in APP processing, while two out of three enzymatic activities of the proteasome increased. Our results are consistent with data showing that soluble Aβ can be degraded by the proteasome. Furthermore, an increase in proteasome function may explain the effects of MB on other proteins inclusions such as TDP-43 and polyglutamine (32,37).

Under the conditions used here, MB did not rescue tau mislocalization and phosphorylation. These data appear to be in contradiction with earlier studies showing that MB can alter tau aggregation *in vitro* (35). However, it should be noted that these *in vitro* results were obtained using very high concentrations of MB, which showed to reduce tau aggregation and not phosphorylation (35). Here we could not assess the effects of MB on tau aggregation as at the age used, the 3xTg-AD mice have yet to develop tau aggregates. Although, we cannot exclude that increasing the dose and/or the duration of the MB treatment may ameliorate tau pathology, the data presented here is consistent with a recent report showing that MB does not affect abnormal tau phosphorylation in zebrafish (32).

Also consistent with the data presented here, previous reports indicate that decreasing soluble Aβ alone is sufficient to rescue learning and memory in the presence of early tau pathology (2,23). However, we also have shown that after the tau pathology is well established and NFTs are formed, the decrease of soluble Aβ alone is not sufficient to rescue learning and memory (23). While the effects of MB on tau aggregation in mammals remain to be determined, if confirmed in other animal model, our data would suggest that MB treatment may be more beneficial early in the disease process.

Acknowledgments

References

1. Atamna H, Nguyen A, Schultz C, Boyle K, Newberry J, Kato H, Ames BN. Methylene blue delays cellular senescence and enhances key mitochondrial biochemical pathways. Faseb J. 2008; 22(3): 703–12. [PubMed: 17928358]

2. Billings LM, Oddo S, Green KN, McGaugh JL, LaFerla FM. Intraneuronal Abeta causes the onset of early Alzheimer's disease-related cognitive deficits in transgenic mice. Neuron. 2005; 45(5):675–88. [PubMed: 15748844]

3. Bruchey AK, Gonzalez-Lima F. Behavioral, Physiological and Biochemical Hormetic Responses to the Autoxidizable Dye Methylene Blue. American journal of pharmacology and toxicology. 2008; 3(1):72–9. [PubMed: 20463863]

4. Caccamo A, Majumder S, Deng JJ, Bai Y, Thornton FB, Oddo S. Rapamycin rescues TDP-43 mislocalization and the associated low molecular mass neurofilament instability. The Journal of biological chemistry. 2009; 284(40):27416–24. [PubMed: 19651785]

5. Caccamo A, Majumder S, Richardson A, Strong R, Oddo S. Molecular interplay between mammalian target of rapamycin (mTOR), amyloid-beta, and Tau: effects on cognitive impairments. The Journal of biological chemistry. 285(17):13107–20. [PubMed: 20178983]

6. Callaway NL, Riha PD, Bruchey AK, Munshi Z, Gonzalez-Lima F. Methylene blue improves brain oxidative metabolism and memory retention in rats. Pharmacology, biochemistry, and behavior. 2004; 77(1):175–81.

7. Callaway NL, Riha PD, Wrubel KM, McCollum D, Gonzalez-Lima F. Methylene blue restores spatial memory retention impaired by an inhibitor of cytochrome oxidase in rats. Neuroscience letters. 2002; 332(2):83–6. [PubMed: 12384216]

8. Gallagher D, Mhaolain AN, Lawlor B. The imperative for disease modifying treatments in Alzheimer's disease. Irish medical journal. 2009; 102(2):37–8. [PubMed: 19405314]

9. Gura T. Hope in Alzheimer's fight emerges from unexpected places. Nature medicine. 2008; 14(9): 894.

10. Hardy J, Selkoe DJ. The amyloid hypothesis of Alzheimer's disease: progress and problems on the road to therapeutics. Science (New York, NY. 2002; 297(5580):353–6.

11. Hauptmann S, Scherping I, Drose S, Brandt U, Schulz KL, Jendrach M, Leuner K, Eckert A, Muller WE. Mitochondrial dysfunction: an early event in Alzheimer pathology accumulates with age in AD transgenic mice. Neurobiology of aging. 2009; 30(10):1574–86. [PubMed: 18295378]

12. Jinwal UK, Miyata Y, Koren J 3rd, Jones JR, Trotter JH, Chang L, O'Leary J, Morgan D, Lee DC, Shults CL, Rousaki A, Weeber EJ, Zuiderweg ER, Gestwicki JE, Dickey CA. Chemical manipulation of hsp70 ATPase activity regulates tau stability. J Neurosci. 2009; 29(39):12079–88. [PubMed: 19793966]

13. Keller JN, Hanni KB, Markesbery WR. Impaired proteasome function in Alzheimer's disease. Journal of neurochemistry. 2000; 75(1):436–9. [PubMed: 10854289]

14. Necula M, Breydo L, Milton S, Kayed R, van der Veer WE, Tone P, Glabe CG. Methylene blue inhibits amyloid Abeta oligomerization by promoting fibrillization. Biochemistry. 2007; 46(30): 8850–60. [PubMed: 17595112]

15. Oddo S. The ubiquitin-proteasome system in Alzheimer's disease. Journal of cellular and molecular medicine. 2008; 12(2):363–73. [PubMed: 18266959]

16. Oddo S, Billings L, Kesslak JP, Cribbs DH, LaFerla FM. Abeta immunotherapy leads to clearance of early, but not late, hyperphosphorylated tau aggregates via the proteasome. Neuron. 2004; 43(3):321–32. [PubMed: 15294141]

17. Oddo S, Caccamo A, Cheng D, Jouleh B, Torp R, LaFerla FM. Genetically augmenting tau levels does not modulate the onset or progression of Abeta pathology in transgenic mice. Journal of neurochemistry. 2007; 102(4):1053–63. [PubMed: 17472708]

18. Oddo S, Caccamo A, Green KN, Liang K, Tran L, Chen Y, Leslie FM, LaFerla FM. Chronic nicotine administration exacerbates tau pathology in a transgenic model of Alzheimer's disease. Proceedings of the National Academy of Sciences of the United States of America. 2005; 102(8): 3046–51. [PubMed: 15705720]

19. Oddo S, Caccamo A, Shepherd JD, Murphy MP, Golde TE, Kayed R, Metherate R, Mattson MP, Akbari Y, LaFerla FM. Triple-transgenic model of Alzheimer's disease with plaques and tangles: intracellular Abeta and synaptic dysfunction. Neuron. 2003; 39(3):409–21. [PubMed: 12895417]

20. Oddo S, Caccamo A, Smith IF, Green KN, LaFerla FM. A dynamic relationship between intracellular and extracellular pools of Abeta. The American journal of pathology. 2006; 168(1): 184–94. [PubMed: 16400022]

21. Oddo S, Caccamo A, Tran L, Lambert MP, Glabe CG, Klein WL, LaFerla FM. Temporal profile of amyloid-beta (Abeta) oligomerization in an in vivo model of Alzheimer disease. A link between Abeta and tau pathology. The Journal of biological chemistry. 2006; 281(3):1599–604. [PubMed: 16282321]

22. Oddo S, Caccamo A, Tseng B, Cheng D, Vasilevko V, Cribbs DH, LaFerla FM. Blocking Abeta42 accumulation delays the onset and progression of tau pathology via the C terminus of heat shock protein70-interacting protein: a mechanistic link between Abeta and tau pathology. J Neurosci. 2008; 28(47):12163–75. [PubMed: 19020010]

23. Oddo S, Vasilevko V, Caccamo A, Kitazawa M, Cribbs DH, LaFerla FM. Reduction of soluble Abeta and tau, but not soluble Abeta alone, ameliorates cognitive decline in transgenic mice with plaques and tangles. The Journal of biological chemistry. 2006; 281(51):39413–23. [PubMed: 17056594]

24. Ohsumi Y. Molecular dissection of autophagy: two ubiquitin-like systems. Nat Rev Mol Cell Biol. 2001; 2(3):211–6. [PubMed: 11265251]

25. Oz M, Lorke DE, Hasan M, Petroianu GA. Cellular and molecular actions of methylene blue in the nervous system. Medicinal research reviews. 2009

26. Panduri V, Surapureddi S, Soberanes S, Weitzman SA, Chandel N, Kamp DW. P53 mediates amosite asbestos-induced alveolar epithelial cell mitochondria-regulated apoptosis. American journal of respiratory cell and molecular biology. 2006; 34(4):443–52. [PubMed: 16357363]

27. Peter C, Hongwan D, Kupfer A, Lauterburg BH. Pharmacokinetics and organ distribution of intravenous and oral methylene blue. European journal of clinical pharmacology. 2000; 56(3): 247–50. [PubMed: 10952480]

28. Pickford F, Masliah E, Britschgi M, Lucin K, Narasimhan R, Jaeger PA, Small S, Spencer B, Rockenstein E, Levine B, Wyss-Coray T. The autophagy-related protein beclin 1 shows reduced expression in early Alzheimer disease and regulates amyloid beta accumulation in mice. The Journal of clinical investigation. 2008; 118(6):2190–9. [PubMed: 18497889]

29. Querfurth HW, LaFerla FM. Alzheimer's disease. The New England journal of medicine. 362(4): 329–44. [PubMed: 20107219]

30. Reddy PH. Role of mitochondria in neurodegenerative diseases: mitochondria as a therapeutic target in Alzheimer's disease. CNS spectrums. 2009; 14(8 Suppl 7):8–13. discussion 6–8. [PubMed: 19890241]

31. Tseng BP, Green KN, Chan JL, Blurton-Jones M, LaFerla FM. Abeta inhibits the proteasome and enhances amyloid and tau accumulation. Neurobiology of aging. 2008; 29(11):1607–18. [PubMed: 17544172]

32. van Bebber F, Paquet D, Hruscha A, Schmid B, Haass C. Methylene blue fails to inhibit Tau and polyglutamine protein-dependent toxicity in zebrafish. Neurobiology of disease.

33. Wang AM, Morishima Y, Clapp KM, Peng HM, Pratt WB, Gestwicki JE, Osawa Y, Lieberman AP. Inhibition of Hsp70 by methylene blue affects signaling protein function and ubiquitination and modulates polyglutamine protein degradation. The Journal of biological chemistry.

34. Wilcock DM, Colton CA. Anti-amyloid-beta immunotherapy in Alzheimer's disease: relevance of transgenic mouse studies to clinical trials. J Alzheimers Dis. 2008; 15(4):555–69. [PubMed: 19096156]

35. Wischik CM, Edwards PC, Lai RY, Roth M, Harrington CR. Selective inhibition of Alzheimer disease-like tau aggregation by phenothiazines. Proceedings of the National Academy of Sciences of the United States of America. 1996; 93(20):11213–8. [PubMed: 8855335]

36. Woodruff-Pak DS. Animal models of Alzheimer's disease: therapeutic implications. J Alzheimers Dis. 2008; 15(4):507–21. [PubMed: 19096153]

37. Yamashita M, Nonaka T, Arai T, Kametani F, Buchman VL, Ninkina N, Bachurin SO, Akiyama H, Goedert M, Hasegawa M. Methylene blue and dimebon inhibit aggregation of TDP-43 in cellular models. FEBS letters. 2009; 583(14):2419–24. [PubMed: 19560462]

38. Yao J, Irwin RW, Zhao L, Nilsen J, Hamilton RT, Brinton RD. Mitochondrial bioenergetic deficit precedes Alzheimer's pathology in female mouse model of Alzheimer's disease. Proceedings of the National Academy of Sciences of the United States of America. 2009; 106(34):14670–5. [PubMed: 19667196]

39. Zheng Y, Shi Y, Tian C, Jiang C, Jin H, Chen J, Almasan A, Tang H, Chen Q. Essential role of the voltage-dependent anion channel (VDAC) in mitochondrial permeability transition pore opening and cytochrome c release induced by arsenic trioxide. Oncogene. 2004; 23(6):1239–47. [PubMed: 14647451]
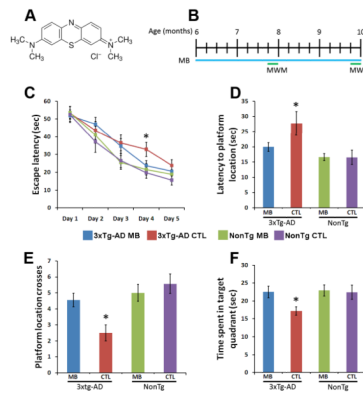
Figure 1. MB rescues early learning and memory deficits in 3xTg-AD mice
(A) Chemical structure of Methylene blue. (B) Schematic of the treatment paradigm. 6-month-old 3xTg-AD (n=17) and NonTg (n=13) mice were treated with MB (0.025% w/w) supplemented diet provided *ad libitum* for 16 weeks. Additionally, age- and sex-matched 3xTg-AD (n=14) and NonTg (n=10) mice were given the control diet. Mice were evaluated in the spatial reference version of the Morris water maze during week 8 and 16. (C) All groups improved over 5 days of training. However, escape latency was significantly reduced in the MB-treated 3xTg-AD mice compared to the 3xTg-AD mice on the control diet (p<0.05). (D–F) Reference memory, measured 24 hours after the last training trial, was significantly improved in the MB-treated 3xTg-AD mice compared to 3xTg-AD mice on the control diet. Notably, MB-treated 3xTg-AD mice performed as well as both NonTg mice. Data are presented as means ± SEM and were analyzed using one-way ANOVA following by post hoc Bonferroni test to determine individual differences in groups. * indicates p<0.05.
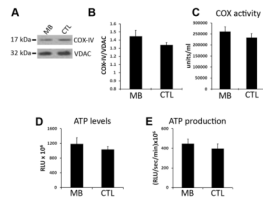
**Figure 2. MB does not significantly increase mitochondrial function**
(A) Representative Western blots of protein obtained from a mitochondrial enriched fraction from brains of MB-treated (n=6) and control 3xTg-AD (n=5) mice and probed with COX-IV and VDAC antibodies as a loading control. (B) Densitometric analysis of the blots revealed no significant change in the COX-IV levels. (C) No changes in cytochrome c oxidase activity were observed in MB-treated 3xTg-AD mice (n=17) compared to 3xTg-AD mice (n=12) on the control diet. (D) ATP levels were measured in the cytosolic fraction and no significant changes were observed in MB-treated 3xTg-AD mice (n=17) compared to 3xTg-AD mice on the control diet (n=13). (E) Kinetic readings were taken to measure ATP production in the mitochondrial enriched fraction energized with glutamate and malate by luciferase assay. ATP production rates were not significantly changed in MB-treated 3xTg-AD mice (n=15) compared to 3xTg-AD mice on the control diet (n=11). Data were analyzed using t-test analysis.
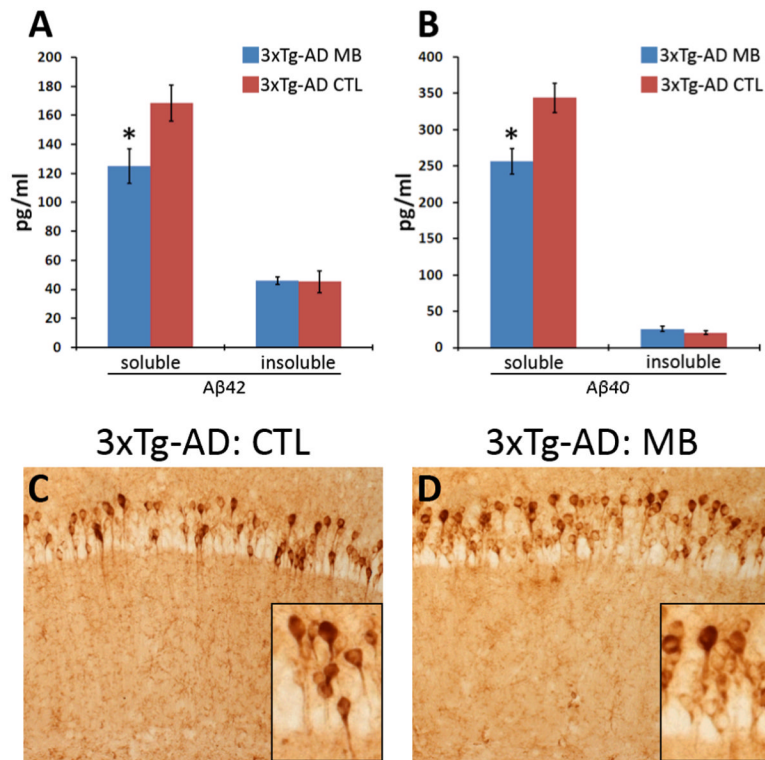
Figure 3. MB reduces Aβ levels in 3xTg-AD mice
(A–B) MB significantly decreased soluble $A\beta_{42}$ and $A\beta_{40}$ levels as measured by ELISA. Data obtained from 12 3xTg-AD on MB and 7 3xTg-AD on the control diet. (C–D) Representative microphotographs depicting CA1 pyramidal neurons of MB-treated and untreated 3xTg-AD stained with 6E10 antibody. Notably, these results were also confirmed with Aβ42 specific antibodies. Sections from 5 different 3xTg-AD mice on MB were compared to sections from 5 different 3xTg-AD on the control diet. Inserts represent higher magnification views of panels C and D. Data are presented as ± SEM and analyzed by t-test analysis. * indicates $p<0.05$.
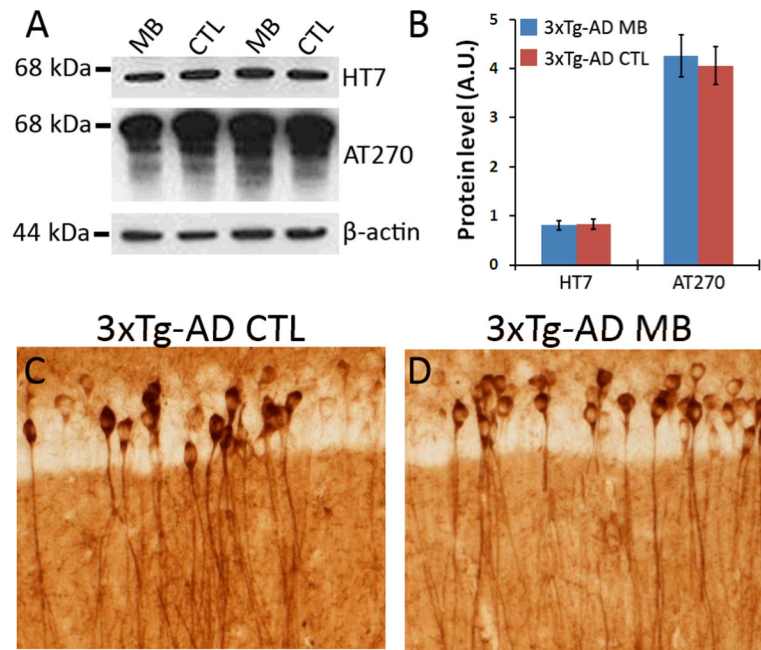
Figure 4. MB does not affect tau pathology in 3xTg-AD

(A) Representative Western blots of proteins extracted from brains of 3xTg-AD mice and probed with human tau specific antibody HT7, phospho-specific antibody AT270 (which recognize tau phosphorylated at Thr181) with β-actin as a loading control. (B) Densitometric analysis of blots (normalized to β-actin) indicates that MB has no effect on tau accumulation or phosphorylation. Data obtained from 5 treated and 5 untreated 3xTg-AD mice. (C–D) Representative microphotographs of CA1 pyramidal neurons stained with anti-tau antibody HT7 indicate that MB does not alter tau mislocalization. 5 mice/treatment were analyzed. Data are presented as ± SEM and analyzed by t-test analysis.
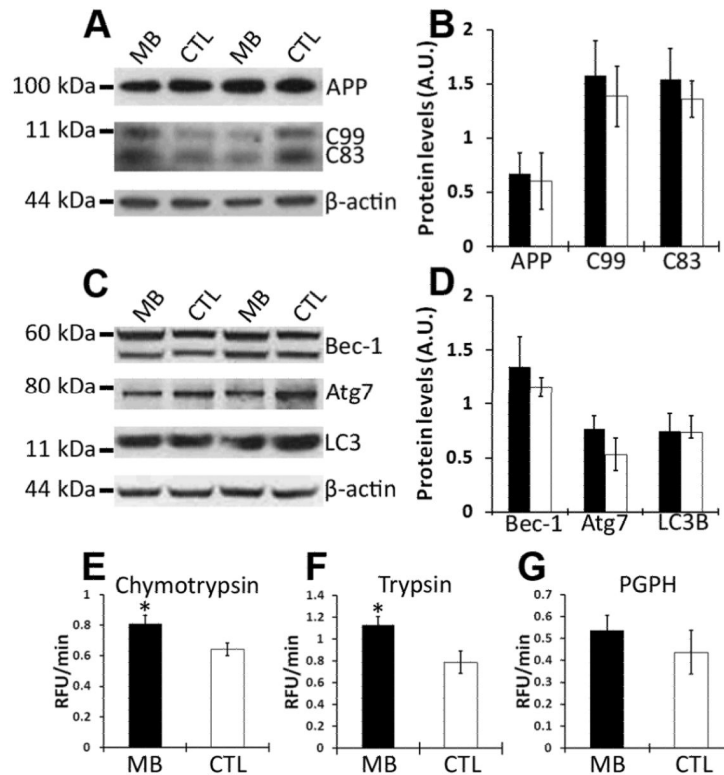
Figure 5. MB increases proteasome activity
(A) Representative Western blots of proteins extracted from brains of MB-treated and control 3xTg-AD mice probed with antibodies 6E10, CT20, and β-actin as a loading control. (B) Densitometric analysis of blots (normalized to β-actin) indicates that the steady-state levels of APP and the two major c-terminal fragments (C99 and C83) were not affected by MB treatment. Data obtained from 5 treated and 5 untreated 3xTg-AD mice. (C) Representative Western blots of proteins extracted from brains of MB treated and control 3xTg-AD mice probed with different autophagy markers. (D) Densitometric analysis indicates that MB does not significantly affect the steady-state levels of Beclin-1, ATG-7, or LC3B. Data obtained from 5 treated and 5 untreated 3xTg-AD mice. (E–G) Brain homogenates from MB-treated (n=12) and control (n=6) 3xTg-AD mice were analyzed for proteasome activity. The data show that MB increases the chymotrypsin- and trypsin- like activity, while it has no effect on the peptidylglutamyl-peptide hydrolyzing (PDPH) activity. Data are presented as means ± SEM and analyzed by t-test analysis. Abbreviation: Bec-1: Beclin 1. * indicates p<0.05.

Table 1

Percent of body weight change during Methylene Blue administration

The table shows the average body weight of each group of mice per each week of treatment. Weights were not taken on week 9 or 14.

Mice	Treatment	1	% Weight Change during the 16 weeks of treatment													
			2	3	4	5	6	7	8	10	11	12	13	15	16
3xTg-AD (n=17)	MB	0	−0.02 +/− 2.22%	−0.82 +/− 2.11%	1.44 +/− 2.26%	−1.88 +/− 1.81%	2.30 +/− 1.42%	1.84 +/− 1.58%	1.56 +/− 1.35%	1.66 +/− 1.10%	2.94 +/− 0.99%	3.36 +/− 1.11%	4.74 +/− 1.41%	4.00 +/− 1.18%	5.08 +/− 1.44%
3xTg-AD (n=14)	CTL	0	−6.05 +/− 3.50%	−0.48 +/− 3.89%	−2.53 +/− 2.84%	−2.48 +/− 4.02%	0.60 +/− 4.46%	1.13 +/− 4.60%	0.87 +/− 4.79%	0.29 +/− 4.79%	1.06 +/− 4.03%	0.84 +/− 4.55%	0.99 +/− 4.62%	−1.83 +/− 3.68%	0.53 +/− 3.43%
NonTg (n=13)	MB	0	0.48 +/− 3.11%	0.20 +/− 1.84%	0.58 +/− 1.84%	1.51 +/− 1.63%	−0.35 +/− 1.77%	0.73 +/− 1.76%	−0.68 +/− 1.92%	0.28 +/− 1.34%	0.48 +/− 1.15%	−1.34 +/− 1.3%	0.30 +/− 1.66%	1.11 +/− 1.60%	1.36 +/− 1.64%
NonTg (n=10)	CTL	0	3.15 +/− 1.88%	2.65 +/− 1.64%	−0.37 +/− 7.32%	3.35 +/− 2.16%	4.72 +/− 2.47%	6.90 +/− 2.80%	5.76 +/− 2.70%	6.76 +/− 2.53%	6.53 +/− 2.30%	5.66 +/− 2.65%	6.50 +/− 2.80%	6.56 +/− 2.79%	7.17 +/− 2.79